Mathematical Modelling and Analysis Publisher: Taylor&Francis and VGTU
Volume 22 Number 6, November 2017, 785–808 http://www.tandfonline.com/TMMA
https://doi.org/10.3846/13926292.2017.1381863 ISSN: 1392-6292

eISSN: 1648-3510

H_2 Optimal Model Reduction of Coupled Systems on the Grassmann Manifold *

Ping Yang[a] and Yao-Lin Jiang[a,b]

[a] *College of Mathematics and Systems Science,*
Xinjiang University, 830046 Urumuqi, China
[b] *School of Mathematics and Statistics,*
Xi'an Jiaotong University, Xi'an,710049 Shaanxi, China
E-mail(*corresp.*): yljiang@mail.xjtu.edu.cn

Received December 7, 2017; revised September 13, 2017; published online November 15, 2017

Abstract. In this paper, we focus on the H_2 optimal model reduction methods of coupled systems and ordinary differential equation (ODE) systems. First, the ε-embedding technique and a stable representation of an unstable differential algebraic equation (DAE) system are introduced. Next, some properties of manifolds are reviewed and the H_2 norm of ODE systems is discussed. Then, the H_2 optimal model reduction method of ODE systems on the Grassmann manifold is explored and generalized to coupled systems. Finally, numerical examples demonstrate the approximation accuracy of our proposed algorithms.

Keywords: model reduction, H_2 optimality, coupled systems, manifolds.

AMS Subject Classification: 78M34; 14M15.

1 Introduction

Lots of large-scale or complex dynamical systems are involved in many engineering application fields, such as electronic systems, control systems, mechanical systems. Generally, the more detailed description is used in these fields, the more complex dynamical systems are established, which imply some difficulties in system control and simulation due to the large size of systems. Fortunately, model reduction provides a way to deal with these difficulties. It approximates the large-scale system by a significantly lower-order system, which can efficiently reduce the complexity of computation and analysis [3,11].

Many model reduction methods have been proposed in the last few decades, such as Krylov subspace model reduction methods [18,25], orthogonal polynomial model reduction methods [13,14,21], the proper orthogonal decomposition

* This work was supported by the Natural Science Foundation of China (Grant Nos. 61663043 and 11371287) and the Doctoral Innovation Project of Xinjiang University (Grant No. XJUBSCX-2016005).

(POD) [10, 17] and H_2 optimal model reduction methods [6, 8]. For the last method, it is worth mentioning that by seeking the reduced system such that the error between the original system and the reduced system in the meaning of the H_2 norm is as small as possible, the model reduction error can be measured. Concerning the H_2 optimal model reduction, there are many researchers devoting to this field. Some norms for both continous-time and discrete-time DAE systems were studied in [26]. [25] indicated that by picking enough initial shifts to be mirror images of the poles of the unstable system, the iterative rational Krylov algorithm (IRKA) converges and also captures the unstable poles. Magruder et al. generalized the Meier-Luenberger interpolation conditions for H_2 optimal approximation of stable dynamical systems to unstable systems without purely imaginary poles [18]. [9] extended the IRKA method proposed in [8] to DAE systems. Moreover, Vuillemin et al. investigated the optimal frequency-limited H_2 model reduction methods for linear time invariant systems [28,29,30]. In addition, Panzer et al. established H_2 and H_∞ error bounds for model reduction of second order systems by Krylov subspace methods [20]. Since the transfer function of the reduced system is only related to the subspaces spanned by the transformation matrices, the H_2 model reduction error is seen as the cost function defined on the Grassmann manifold, and the H_2 optimal model reduction problem is treated as a minimization problem on the Grassmann manifold. Then some optimization techniques are employed to solve the minimization problem [15, 32].

Coupled systems often consist of ODE subsystems and DAE subsystems, such as very large system integrated (VLSI) designs, micro-electro-mechanical systems (MEMS), and the spatial discretization of some partial differential equations (PDEs). As we know, ODE systems have been explored extensively, while DAE systems relatively less. [5, 12] indicated that by embedding a small perturbation in a DAE system, a corresponding ODE system can be obtained. Then these existing model reduction methods for ODE systems can be employed. When the perturbation is small enough, the ODE system can approximate the DAE system well. As to an unstable DAE system, [24] introduced a means to transform the unstable system into a coupled system with stable subsystems, and it is equipped with the same transfer function.

In this paper, based on the Grassmann manifold, we investigate H_2 optimal model reduction of the coupled system with unstable subsystems. First, the ε-embedding technique and the stable representation of the unstable DAE system are introduced. Next, we explore the H_2 optimal model reduction of ODE systems and it leads to the H_2 optimal model reduction on the Grassmann manifold. Then, the ε-embedding technique is applied to the DAE subsystems such that all of the subsystems of the given coupled system are ODE subsystems. In order to ensure the stability of subsystems and the closed-loop system, the stable representations of unstable subsystems and the unstable closed-loop system are generated. Finally, the algorithm is extended to the coupled system and two model reduction algorithms are presented. One reduces the order of the closed-loop system, while the other is adaptive to subsystems of the coupled system in order to preserve the interconnected relations.

The reminder of this paper is organized as below. In Section 2, coupled systems and DAE systems are briefly reviewed. In Section 3, the ε-embedding technique and the stable representation of the unstable DAE system are discussed. H_2 optimal model reduction for ODE systems based on the Grassmann manifold is investigated in Section 4 while two model reduction algorithms for coupled systems are presented in Section 5. Two numerical examples resulting from the spatial descretization of PDEs are given in Section 6 to illustrate the accuracy of proposed algorithms. Finally, some conclusions are drawn in Section 7.

2 Preliminary results

The ith subsystem of the coupled system is described as follows

$$\begin{cases} E_i \dfrac{dx_i(t)}{dt} = A_i x_i(t) + B_i u_i(t), \\ y_i(t) = C_i x_i(t), \end{cases} \tag{2.1}$$

where $E_i, A_i \in \mathbf{R}^{n_i \times n_i}$, $B_i \in \mathbf{R}^{n_i \times p_i}$, $C_i \in \mathbf{R}^{m_i \times n_i}$, $x_i(t) \in \mathbf{R}^{n_i}$ is the state vector, $u_i(t) \in \mathbf{R}^{p_i}$ is the internal input vector, $y_i(t) \in \mathbf{R}^{m_i}$ is the internal output vector, $i = 1, 2, \ldots, k$. We call the system (2.1) is an ODE subsystem if $\mathrm{rank}(E_i) = n_i$, and a DAE subsystem, otherwise. When the initial state vector $x_i(0) = 0$, the transfer function of the subsystem (2.1) is $H_i(s) = C_i(sE_i - A_i)^{-1}B_i$. The controllability Gramian P_i and the observability Gramian Q_i satisfy the following generalized Lyapunov equations

$$\begin{aligned} E_i P_i A_i^T + A_i P_i E_i^T + B_i B_i^T = 0, \\ E_i^T Q_i A_i + A_i^T Q_i E_i + C_i^T C_i = 0. \end{aligned}$$

The subsystems are coupled by the following interconnected relations

$$\begin{cases} u_i(t) = K_{i1} y_1(t) + \ldots + K_{ik} y_k(t) + G_i u(t), \\ y(t) = R_1 y_1(t) + \ldots + R_k y_k(t), \end{cases} \tag{2.2}$$

where $K_{il} \in \mathbf{R}^{p_i \times m_l}$, $l = 1, 2, \ldots, k$, $G_i \in \mathbf{R}^{p_i \times p}$, $R_i \in \mathbf{R}^{m \times m_i}$, $u(t) \in \mathbf{R}^p$ is the external input vector, $y(t) \in \mathbf{R}^m$ is the external output vector. (2.1) and (2.2) constitute a coupled system with k subsystems. Let $K = [K_{il}]_{k \times k} \in \mathbf{R}^{p_0 \times m_0}$, $G = [G_1^T \ldots G_k^T]^T \in \mathbf{R}^{p_0 \times p}$, $R = [R_1 \ldots R_k] \in \mathbf{R}^{m \times m_0}$, $\overline{E} = \mathrm{diag}\{E_1, \ldots, E_k\} \in \mathbf{R}^{n \times n}$, $\overline{A} = \mathrm{diag}\{A_1, \ldots, A_k\} \in \mathbf{R}^{n \times n}$, $\overline{B} = \mathrm{diag}\{B_1, \ldots, B_k\} \in \mathbf{R}^{n \times p_0}$ and $\overline{C} = \mathrm{diag}\{C_1, \ldots, C_k\} \in \mathbf{R}^{m_0 \times n}$, where $n = n_1 + \ldots + n_k$, $p_0 = p_1 + \ldots + p_k$, $m_0 = m_1 + \ldots + m_k$.

Let $\overline{H}(s) = \overline{C}(s\overline{E} - \overline{A})^{-1}\overline{B}$. Obviously, we have $\overline{H}(s) = \mathrm{diag}\{H_1(s), \ldots, H_k(s)\}$. If $I_{m_0} - \overline{H}(s)K$ is invertible, then the transfer function of the coupled system [11] can be written as

$$R(I_{m_0} - \overline{C}(s\overline{E} - \overline{A})^{-1}\overline{B}K)^{-1}\overline{C}(s\overline{E} - \overline{A})^{-1}\overline{B}G = R\overline{C}(s\overline{E} - (\overline{A} + \overline{B}K\overline{C}))^{-1}\overline{B}G,$$

which leads to the following closed-loop system

$$\begin{cases} E_0 \dfrac{dx_0(t)}{dt} = A_0 x_0(t) + B_0 u(t), \\ y_0(t) = C_0 x_0(t), \end{cases} \tag{2.3}$$

where $E_0 = \overline{E} \in \mathbf{R}^{n\times n}$, $A_0 = \overline{A} + \overline{B}K\overline{C} \in \mathbf{R}^{n\times n}$, $B_0 = \overline{B}G \in \mathbf{R}^{n\times p}$, $C_0 = R\overline{C} \in \mathbf{R}^{m\times n}$, $x_0(t) \in \mathbf{R}^n$ is the state vector, $y_0(t) \in \mathbf{R}^m$ is the output vector, and the transfer function can be given by $H_0(s) = C_0(sE_0 - A_0)^{-1}B_0$. If a system has the same transfer function as the system (2.3), we call these two systems are equivalent.

Whether the subsystems of the coupled system or the closed-loop system can be written as the following form

$$\begin{cases} E\dfrac{dx(t)}{dt} = Ax(t) + Bu(t), \\ y(t) = Cx(t), \end{cases} \tag{2.4}$$

where $E, A \in \mathbf{R}^{n\times n}$, $B \in \mathbf{R}^{n\times p}$, $C \in \mathbf{R}^{m\times n}$. We consider the transfer function of the system (2.4) given by $H(s) = C(sE - A)^{-1}B$. P and Q are the controllability Gramian and the observability Gramian of (2.4).

We seek a transformation matrix $V \in \mathbf{R}^{n\times r}$ such that $V^TV = I_r$ and $r \ll n$. The reduced system can be constructed as

$$\begin{cases} \widetilde{E}\dfrac{d\tilde{x}(t)}{dt} = \widetilde{A}\tilde{x}(t) + \widetilde{B}u(t), \\ \tilde{y}(t) = \widetilde{C}\tilde{x}(t), \end{cases} \tag{2.5}$$

where $\widetilde{E} = V^TEV \in \mathbf{R}^{r\times r}$, $\widetilde{A} = V^TAV \in \mathbf{R}^{r\times r}$, $\widetilde{B} = V^TB \in \mathbf{R}^{r\times p}$, $\widetilde{C} = CV \in \mathbf{R}^{m\times r}$. The transfer function of the system (2.5) can be given by $\widetilde{H}(s) = \widetilde{C}(s\widetilde{E} - \widetilde{A})^{-1}\widetilde{B}$. The controllability Gramian $\widetilde{P}$ and the observability Gramian $\widetilde{Q}$ individually satisfy the following generalized Lyapunov equations

$$\widetilde{E}\widetilde{P}\widetilde{A}^T + \widetilde{A}\widetilde{P}\widetilde{E}^T + \widetilde{B}\widetilde{B}^T = 0, \tag{2.6}$$

$$\widetilde{E}^T\widetilde{Q}\widetilde{A} + \widetilde{A}^T\widetilde{Q}\widetilde{E} + \widetilde{C}^T\widetilde{C} = 0. \tag{2.7}$$

If (2.4) is a improper DAE system, the transfer function has a polynomial part, which has to be exactly matched by that of the reduced system, or the unbounded error will occur as $s \to \infty$ [9]. For simplicity, when the system (2.4) represents a DAE system in the sequel, we always assume it is strictly proper.

In order to analyze the H_2 error between the system (2.4) and the system (2.5), we consider the following error system

$$\begin{cases} \widehat{E}\dfrac{d\hat{x}(t)}{dt} = \widehat{A}\hat{x}(t) + \widehat{B}u(t), \\ \hat{y}(t) = \widehat{C}\hat{x}(t), \end{cases} \tag{2.8}$$

where

$$\widehat{E} = \begin{bmatrix} E & 0 \\ 0 & \widetilde{E} \end{bmatrix}, \quad \widehat{A} = \begin{bmatrix} A & 0 \\ 0 & \widetilde{A} \end{bmatrix}, \quad \widehat{B} = \begin{bmatrix} B \\ \widetilde{B} \end{bmatrix},$$

$$\widehat{C} = \begin{bmatrix} C & -\widetilde{C} \end{bmatrix}, \quad \hat{x}(t) = \begin{bmatrix} x(t) \\ \tilde{x}(t) \end{bmatrix}, \quad \hat{y}(t) = y(t) - \tilde{y}(t).$$

We can consider the transfer function of the error system (2.8) given by $\widehat{H}(s) = \widehat{C}(s\widehat{E} - \widehat{A})^{-1}\widehat{B}$. From the partitioning of the coefficient matrices, we have $\widehat{H}(s) = H(s) - \widetilde{H}(s)$. For the further analysis, partition the controllability Gramian $\widehat{P}$ and the observability Gramian $\widehat{Q}$ as

$$\widehat{P} = \begin{bmatrix} P & X \\ X^T & \widetilde{P} \end{bmatrix}, \quad \widehat{Q} = \begin{bmatrix} Q & Y \\ Y^T & \widetilde{Q} \end{bmatrix} \tag{2.9}$$

conformably with the partitioning of the matrix $\widehat{A}$. Substituting (2.9) into the generalized Lyapunov equations satisfied by $\widehat{P}$ and $\widehat{Q}$, it yields that

$$EX\widetilde{A}^T + AX\widetilde{E}^T + B\widetilde{B}^T = 0, \tag{2.10}$$

$$E^TY\widetilde{A} + A^TY\widetilde{E} - C^T\widetilde{C} = 0. \tag{2.11}$$

In the next two sections the model reduction method for the system (2.4) is investigated. Then, we generalize it to the coupled system in Section 5.

3 The ε-embedding technique and the stable representation of the DAE system

In this section, we present two measures for dealing with the DAE system (2.4). One embeds a small perturbation into the system (2.4) to turn the DAE system into an ODE system. The other is to transform the unstable DAE system into a coupled system with stable subsystems. It has the same transfer function and the same state space dimension as the DAE system.

3.1 On the ε-embedding technique of the DAE system

The DAE system is an important system description in many engineering fields, such as circuits simulation, elastic multibody systems. However, model reduction methods for ODE systems are investigated relatively more. For some existing references dealing with DAE systems, one can refer to [9, 19, 23]. Apart from these, [5] proposed the ε-embedding technique to transform a DAE system into an ODE system by embedding a small perturbation. Then some model reduction methods concerning ODE systems are adaptable to the embedding system.

We consider the system (2.4) with $\mathrm{rank}(E) < n$, and suppose $\mathrm{rank}(E) = l$. By the singular value decomposition (SVD) of E, it yields

$$E = \begin{bmatrix} U_1 & U_2 \end{bmatrix} \begin{bmatrix} \Sigma_1 & \\ & 0 \end{bmatrix} \begin{bmatrix} V_1^T \\ V_2^T \end{bmatrix},$$

where $\Sigma_1 \in \mathbf{R}^{l\times l}$, $U_1, V_1 \in \mathbf{R}^{n\times l}$, $U_2, V_2 \in \mathbf{R}^{n\times(n-l)}$, $[\, U_1 \; U_2 \,]$ and $[\, V_1 \; V_2 \,]$ are two orthogonal matrices. We embed a small perturbation $1 \gg \varepsilon > 0$ in E as

$$E_\varepsilon = \begin{bmatrix} U_1 & U_2 \end{bmatrix} \begin{bmatrix} \Sigma_1 & \\ & \varepsilon I_{n-l} \end{bmatrix} \begin{bmatrix} V_1^T \\ V_2^T \end{bmatrix},$$

which is a nonsingular matrix. Since $\|E_\varepsilon - E\|_2 = \varepsilon$, when ε is small enough, E_ε can approximate E well. For large-scale problems, it may be intractable to perform the SVD on E. A remedy is that some practical applications often lead to the sparsity of (2.4), such as electrical circuit simulations, multibody dynamics, and semidiscretized partial differential equations. [22] investigated efficient algorithms for the sparse SVD. Furthermore, we establish the following system to approximate the DAE system (2.4):

$$\begin{cases} E_\varepsilon \dfrac{dx(t)}{dt} = Ax(t) + Bu(t), \\ y(t) = Cx(t). \end{cases} \tag{3.1}$$

Except for E_ε, all conditions are the same as the system (2.4) and the transfer function of the system (3.1) is $H_\varepsilon(s) = C(sE_\varepsilon - A)^{-1}B$. Before deriving the error between $H(s)$ and $H_\varepsilon(s)$, we present the following lemma.

Lemma 1. *If* $|s| < \min\{\frac{1}{\varepsilon\|A^{-1}\|_2 + \|A^{-1}E\|_2}, \frac{1}{\|A^{-1}E\|_2}\}$, *then*

$$\|(sE_\varepsilon - A)^{-1}\|_2 \le \frac{\|(sE - A)^{-1}\|_2}{1 - \varepsilon|s|\|(sE - A)^{-1}\|_2}.$$

Proof. When $\|sA^{-1}E\|_2 < 1$, i.e., $|s| < \frac{1}{\|A^{-1}E\|_2}$, it holds that

$$\begin{aligned} 1 - \varepsilon|s|\|(sE - A)^{-1}\|_2 &= 1 - \varepsilon|s|\|(I - sA^{-1}E)^{-1}A^{-1}\|_2 \\ &\ge 1 - \varepsilon|s|\|(I - sA^{-1}E)^{-1}\|_2\|A^{-1}\|_2 \ge 1 - \frac{\varepsilon|s|\|A^{-1}\|_2}{1 - |s|\|A^{-1}E\|_2}. \end{aligned}$$

To ensure $1 - \varepsilon|s|\|(sE - A)^{-1}\|_2 > 0$, we just let

$$1 - \frac{\varepsilon|s|\|A^{-1}\|_2}{1 - |s|\|A^{-1}E\|_2} > 0, \quad \text{and} \quad |s| < \frac{1}{\|A^{-1}E\|_2}.$$

That is

$$|s| < \min\left\{\frac{1}{\varepsilon\|A^{-1}\|_2 + \|A^{-1}E\|_2}, \frac{1}{\|A^{-1}E\|_2}\right\}.$$

Since $(sE_\varepsilon - A)^{-1} = (sE - A)^{-1} \sum_{i=0}^{+\infty} (s(E - E_\varepsilon)(sE - A)^{-1})^i$, then

$$\|(sE_\varepsilon - A)^{-1}\|_2 \le \sum_{i=0}^{+\infty} \varepsilon^i |s|^i \|(sE - A)^{-1}\|_2^{i+1} \le \frac{\|(sE - A)^{-1}\|_2}{1 - \varepsilon|s|\|(sE - A)^{-1}\|_2}.$$

Thus, the proof of Lemma 1 is accomplished. □

According to Lemma 1 and the fact that $(sE - A)^{-1} - (sE_\varepsilon - A)^{-1} = s(sE - A)^{-1}(E_\varepsilon - E)(sE_\varepsilon - A)^{-1}$, we can obtain

$$\begin{aligned} \|H(s) - H_\varepsilon(s)\|_2 &= \|C((sE - A)^{-1} - (sE_\varepsilon - A)^{-1})B\|_2 \\ &\le \varepsilon|s|\|C\|_2\|B\|_2\|(sE - A)^{-1}\|_2\|(sE_\varepsilon - A)^{-1}\|_2 \\ &\le \frac{\varepsilon|s|\|C\|_2\|B\|_2\|(sE - A)^{-1}\|_2^2}{1 - \varepsilon|s|\|(sE - A)^{-1}\|_2}, \end{aligned}$$

which implies that when the perturbation ε is sufficiently small, the system (3.1) can well approximate the system (2.4) in the frequency domain.

For convenience, we perform the SVD of E to embed the perturbation in this paper. There is another way called Weierstrass-Kronecker canonical form [16], which is stated in the following remark.

Remark 1. Suppose the matrix pencil (E, A) is regular, i.e., there exists $\lambda \in \mathbf{C}$ such that $\det(\lambda E - A) \neq 0$. Then the matrices E and A can be transformed into the following block diagonal matrices

$$T_l E T_r = \begin{bmatrix} I_{\hat{n}_1} & \\ & \widehat{N} \end{bmatrix}, \quad T_l A T_r = \begin{bmatrix} \widehat{M} & \\ & I_{\hat{n}_2} \end{bmatrix},$$

where $\hat{n}_1 + \hat{n}_2 = n$, $T_l, T_r \in \mathbf{R}^{n\times n}$ are nonsingular, $\widehat{N}$ is a nilpotent matrix and $\widehat{M}$ is a Jordan block.

The embedding process is similar to the above, apart from applying T_l and T_r to transform the system (2.4) before embedding the perturbation ε [12].

3.2 The stable representation of the unstable DAE system

Some practical applications often lead to unstable DAE systems, which can be hardly operated for the unbounded H_2 norm. Even though the IRKA method is generalized to unstable systems, it also has few shortages. For example, when the number of unstable poles of the original system becomes larger, the number of shifts required to match these unstable poles becomes larger as well. A remedy that a stable representation can be constructed by a state feedback matrix is introduced in [4, 24], and here we briefly discuss it.

Let Γ be a given region of the complex plane, $H(s)$ is Γ-stable if all its poles lie in Γ. If $\mathrm{rank}([A^T - sE^T \ C^T]^T) = n$ for arbitrary $s \in \Gamma$, (2.4) is Γ-detectable. For the rational function matrix $H(s)$, if there are Γ-stable rational function matrices $D_1(s)$, $D_2(s)$, $\check{H}_1(s)$ and $\check{H}_2(s)$ such that $D_1(s)\check{H}_1(s) + D_2(s)\check{H}_2(s) = I$, then the factorization $H(s) = \check{H}_1(s)(\check{H}_2(s))^{-1}$ is called as a right coprime factorization (RCF). For any rational transfer function matrix $H(s)$ with a Γ-stabilizable and Γ-detectable realization, the RCF can be obtained by the following factors

$$\begin{bmatrix} \check{H}_1(s) \\ \check{H}_2(s) \end{bmatrix} = \begin{bmatrix} C \\ F \end{bmatrix} (sE - A - BF)^{-1} B + \begin{bmatrix} 0 \\ I \end{bmatrix}, \tag{3.2}$$

where $F \in \mathbf{R}^{p\times n}$ is a state feedback matrix such that all finite eigenvalues of the matrix pencil $(A + BF, E)$ lie in Γ. For the computation of the feedback matrix F, [27] provided the GRCF-PD algorithm. When Γ stands for the open left half plane, it yields a stable representation of the unstable DAE system.

According to (3.2), the extended transfer function

$$\check{H}_{new}(s) = \begin{bmatrix} \check{H}_1(s) \\ \check{H}_2(s) - I \end{bmatrix}$$

is stable and has the generalized state space realization

$$\begin{cases} E\dot{x}(t) = (A+BF)x(t) + Bv(t), \\ \begin{bmatrix} y_1(t) \\ y_2(t) \end{bmatrix} = \begin{bmatrix} C \\ F \end{bmatrix} x(t). \end{cases} \tag{3.3}$$

To ensure the same transfer function, (3.3) couples with the following interconnected relations

$$\begin{cases} v(t) = -y_2(t) + u(t) = \begin{bmatrix} 0 & -I \end{bmatrix} \begin{bmatrix} y_1(t) \\ y_2(t) \end{bmatrix} + u(t), \\ y(t) = y_1(t) = \begin{bmatrix} I & 0 \end{bmatrix} \begin{bmatrix} y_1(t) \\ y_2(t) \end{bmatrix}. \end{cases} \tag{3.4}$$

We know that the system (3.3) and the relations (3.4) make up a coupled system, which has the same transfer function as the system (2.4). Furthermore, the order of the system (3.3) is still n, so transforming the system (2.4) into a coupled system does not enlarge the size of the state space.

Remark 2. The system (3.3) implies that the stable representation does not change the coefficient matrix E, so if the system (2.4) is a DAE system, the subsystem of the new coupled system is still a DAE subsystem.

What should be noticed is that when we transform an unstable subsystem of the coupled system into a coupled system with stable subsystems, the internal input, the internal output and the interconnected relations accordingly changed, so the corresponding modifications should be done.

Suppose the ith subsystem of the coupled system is unstable. We can construct a state feedback matrix F_i. Let $\check{H}_{i1}(s) = C_i(sE_i - A_i - B_iF_i)^{-1}B_i$, and $\check{H}_{i2}(s) = F_i(sE_i - A_i - B_iF_i)^{-1}B_i + I_{n_i}$. Then the subsystem is replaced by a new coupled system (3.3) and (3.4) with the subscript i. Accordingly, the original coupled relations (2.2) yield

$$\begin{cases} v_i(t) = -y_{2i}(t) + u_i(t) = -y_{2i}(t) + K_{i1}y_1(t) + \ldots + K_{ik}y_k(t) + G_iu(t), \\ y(t) = R_1y_1(t) + \ldots + R_iy_{i1}(t) + \ldots + R_ky_k(t). \end{cases}$$

The closed-loop transfer function of the new extended coupled system is given by $H_{new,0}(s) = R_{new}(I - \overline{H}_{new}(s)K_{new})^{-1}\overline{H}_{new}(s)G$, where

$$\begin{aligned} K_{new} &= K\text{diag}\{I, \ldots, I, [I_{m_i}, 0], I, \ldots, I\} - \text{diag}\{0, \ldots, 0, [0, I_{p_i}], 0, \ldots, 0\}, \\ R_{new} &= [\ R_1, \ldots, R_{i-1}, R_i, 0, R_{i+1}, \ldots, R_k\ ], \\ \overline{H}_{new}(s) &= \text{diag}\{H_1(s), \ldots, H_{i-1}(s), \check{H}_{new,i}(s), H_{i+1}(s), \ldots, H_k(s)\}. \end{aligned}$$

If the coupled system has more than one unstable subsystem, the above situation can be similarly generalized. When reduce the order of the ith unstable subsystem, we let V_i be the transformation matrix. Then the reduced subsystem of (3.3) can be written as

$$\begin{cases} V_i^T E V_i \dot{\tilde{x}}_i(t) = V_i^T (A+BF) V_i \tilde{x}_i(t) + V_i^T B \tilde{v}_i(t), \\ \begin{bmatrix} \tilde{y}_{1i}(t) \\ \tilde{y}_{2i}(t) \end{bmatrix} = \begin{bmatrix} C \\ F \end{bmatrix} V_i \tilde{x}_i(t) \end{cases} \tag{3.5}$$

and the interconnected relations is given by

$$\begin{cases} \tilde{v}_i(t) = -\tilde{y}_{2i}(t) + \tilde{u}_i(t) = \begin{bmatrix} 0 & -I \end{bmatrix} \begin{bmatrix} \tilde{y}_{1i}(t) \\ \tilde{y}_{2i}(t) \end{bmatrix} + \tilde{u}_i(t), \\ \tilde{y}_i(t) = \tilde{y}_{1i}(t) = \begin{bmatrix} I & 0 \end{bmatrix} \begin{bmatrix} \tilde{y}_{1i}(t) \\ \tilde{y}_{2i}(t) \end{bmatrix}. \end{cases} \tag{3.6}$$

Substituting (3.6) into (3.5), the reduced system of the ith subsystem can be obtained as below

$$\begin{cases} V_i^T E_i V_i \dfrac{d\tilde{x}_i(t)}{dt} = V_i^T A_i V_i \tilde{x}_i(t) + V_i^T B_i \tilde{u}_i(t), \\ \tilde{y}_i(t) = C V_i \tilde{x}_i(t), \end{cases}$$

which indicates that the structure of the coupled system can be preserved.

Taking the measures introduced in this section, we explore the H_2 optimal model reduction of ODE systems on the Grassmann manifold in the next section.

4 H_2 optimal model reduction of the ODE system on the Grassmann manifold

For the system (2.4), when $\operatorname{rank}(E) = n$, it is an ODE system. We firstly introduce the Grassmann manifold and some properties. Then the H_2 norm of the error system is regarded as the cost function defined on the Grassmann manifold. Finally, by some optimization techniques, the model reduction method for minimizing the cost function is investigated.

4.1 The Grassmann manifold

In this subsection, we view the Grassmann manifold as the quotient manifold of the Stiefel manifold, which is an embedded submanifold of the Euclidean space. Then some properties of the quotient manifold and the embedded submanifold are involved.

Let $\mathbf{R}^{n\times r}$ stand for the set of all of $n \times r$ matrices, and it is a manifold [7]. A Stiefel manifold is a subset of $\mathbf{R}^{n\times r}$, which can be written as

$$St(r,n) := \{V : V^T V = I_r, V \in \mathbf{R}^{n\times r}\}.$$

On the Stiefel manifold, we define an equivalence relation that $V_1, V_2 \in St(r,n)$, V_1 is equivalent to V_2, written as $V_1 \sim V_2$, if there is an orthogonal matrix

$M \in \mathbf{R}^{r\times r}$ such that $V_1 = V_2 M$. All of equivalent matrices make up an equivalence class

$$[V] := \{VM : M \in \mathbf{R}^{r\times r}\text{is an orthogonal matrix}\},$$

where V is a presentation of $[V]$. The equivalence relation also defines a division of $St(r,n)$. A set of all of r-dimensional subspaces of $\mathbf{R}^n$ is a Grassmann manifold, written as $Gr(r,n)$, and an element of $Gr(r,n)$ is written as $\mathcal{V}$. For every equivalence class, each of elements in it spans the same subspace. This identifies $Gr(r,n)$ with the quotient space

$$St(r,n)/O_r := \{VO_r : V \in St(r,n)\},$$

where O_r is the set of r-by-r orthogonal matrices. Then we define the natural projection

$$\pi : St(r,n) \to Gr(r,n) : V \mapsto \mathcal{V} = \mathrm{span}(V), \quad \pi^{-1} : \mathcal{V} \mapsto [V].$$

Let $T_V St(r,n)$ and $T_{\mathcal{V}} Gr(r,n)$ be the tangent space of $St(r,n)$ at V and the tangent space of $Gr(r,n)$ at $\mathcal{V}$. We endow every tangent space of $St(r,n)$ with the inner product

$$\langle Z_1, Z_2\rangle_V := 2\mathrm{tr}(Z_1^T Z_2), \quad Z_1, Z_2 \in T_V St(r,n).$$

Similarly, endow every tangent space of $Gr(r,n)$ with the inner product

$$\langle \xi, \eta\rangle_{\mathcal{V}} := 2\mathrm{tr}(\bar{\xi}_V^T \bar{\eta}_V), \quad \xi, \eta \in T_{\mathcal{V}} Gr(r,n),$$

where $\bar{\xi}_V, \bar{\eta}_V \in T_V St(r,n)$ are the horizontal lifts of ξ and η at V such that $D\pi(V)[\bar{\xi}_V] = \xi$ and $D\pi(V)[\bar{\eta}_V] = \eta$, respectively. A manifold endowed with a smoothly varying inner product in tangent spaces is called a Riemannian manifold. Next, we introduce the definition of the gradient [2].

Definition 1. Let J be a smooth real-valued function defined on a Riemannian manifold $\mathcal{M}$. A gradient of J at $\mathcal{V}$, denoted by $\mathrm{grad}J$, is defined as the unique element of $T_{\mathcal{V}}\mathcal{M}$ that satisfies

$$\langle \mathrm{grad}J(\mathcal{V}), \xi\rangle = DJ(\mathcal{V})[\xi], \quad \forall \xi \in T_{\mathcal{V}}\mathcal{M},$$

where $\langle\cdot,\cdot\rangle$ is the inner product of $T_{\mathcal{V}}\mathcal{M}$.

There are some properties of the gradient on $St(r,n)$ and $Gr(r,n)$ mentioned in the following theorem [2].

Theorem 1. *Let $\hat{J}$ be a function defined on $\mathbf{R}^{n\times r}$ and $\tilde{J}$ is the restriction of $\hat{J}$ to $St(r,n)$. Then*

$$\mathrm{grad}\tilde{J}(\widetilde{V}) = \frac{1}{2}(I - \widetilde{V}\widetilde{V}^T)\mathrm{grad}\hat{J}(\widetilde{V}) + \frac{1}{2}\widetilde{V}\mathrm{skew}(\widetilde{V}^T\mathrm{grad}\hat{J}(\widetilde{V})),$$

where $\widetilde{V} \in St(r,n)$ and $\mathrm{skew}(N) := (N - N^T)/2$. Moreover, let J be a function defined on $Gr(r,n)$ such that $\bar{J} = J \circ \pi$. Then the horizontal lift of $\mathrm{grad}J$ at $V \in St(r,n)$ satisfies

$$\overline{\mathrm{grad}J}_V = \mathrm{grad}\bar{J}(V),$$

where $D\pi(V)[\overline{\mathrm{grad}J}_V] = \mathrm{grad}J(V)$.

In order to correlate the tangent space with the Grassmann manifold, we review a theorem about geodesics and horizontal lifts [1].

Theorem 2. *Let $t \mapsto \mathcal{V}(t)$ be a geodesic on $Gr(r,n)$, with $\mathcal{V}(0) = \mathcal{V}_0$, $\xi \in T_{\mathcal{V}_0}Gr(r,n)$. $\mathcal{V}_0 = \pi(V_0)$ and $\bar{\xi}_{V_0}$ is the horizontal lift of ξ at V_0. Then*

$$\mathcal{V}(t) = \mathrm{span}(V_0\overline{V}_0 \cos \overline{\Sigma}_0 t + \overline{U}_0 \sin \overline{\Sigma}_0 t)$$

and $V(t) := (V_0\overline{V}_0 \cos \overline{\Sigma}_0 t + \overline{U}_0 \sin \overline{\Sigma}_0 t)\overline{V}_0^T$ lies in $St(r,n)$, where $\overline{U}_0\overline{\Sigma}_0\overline{V}_0^T$ is the thin SVD of $\bar{\xi}_{V_0}$, that is, $\overline{U}_0 \in \mathbf{R}^{n\times r}$ is an orthonormal matrix, $\overline{V}_0 \in \mathbf{R}^{r\times r}$ is an orthogonal matrix, and $\overline{\Sigma}_0 \in \mathbf{R}^{r\times r}$ is a diagonal matrix with nonnegative elements.

From Theorem 1 and Theorem 2, we can compute the horizontal lift of the gradient instead of the gradient on the Grassmann manifold. Specifically, we can compute the corresponding partial derivative on $\mathbf{R}^{n\times r}$ and project it onto the tangent space of $St(r,n)$.

When the system (2.4) is a DAE system, a corresponding ODE system can be obtained by the ε-embedding technique. In the following subsection, we explore the model reduction method of the ODE system.

4.2 Model reduction of the ODE system

In this subsection, we mainly investigate H_2 optimal model reduction of the ODE system on the Grassmann manifold, and some results are used to generate the corresponding algorithm.

Lemma 2. *Given the stable system (2.4), E is nonsingular. P and Q are the controllability Gramian and the observability Gramian, respectively. Then the H_2 norm of $H(s)$ can be written as*

$$\|H(s)\|_{H_2}^2 = \mathrm{tr}(CPC^T) = \mathrm{tr}(B^TQB).$$

As seen from Lemma 2, the H_2 norm of the error system (2.8) can be written as $\|\widehat{H}(s)\|_{H_2}^2 = \mathrm{tr}(\widehat{C}\widehat{P}\widehat{C}^T) = \mathrm{tr}(\widehat{B}^T\widehat{Q}\widehat{B})$, which is a function regarding the orthonormal matrix V. Let $J(V) := \|\widehat{H}(s)\|_{H_2}^2$. Then $J(V)$ is a cost function defined on $St(r,n)$. In addition, given an arbitrary orthogonal matrix $M \in \mathbf{R}^{r\times r}$, it holds $J(VM) = J(V)$, so $J(V)$ is a cost function defined on $Gr(r,n)$, and $J(V) = J(\mathcal{V}) = J \circ \pi(V)$.

For the system (2.4), when $E = I$, there is an existing model reduction method [32] on the Riemannian manifold, which is stated in the following theorem.

Theorem 3. *Given the stable system (2.4) with $E = I$. $\widetilde{P}$ and $\widetilde{Q}$ are the controllability Gramian and the observability Gramian of the reduced system (2.5). X and Y satisfy (2.10) and (2.11), respectively. Then the partial derivative of $J(V)$ at V is $J_V = 2R$, where*

$$\begin{aligned} R :=& (-C^TC + A^TVY^T)X + (C^TCV + A^TV\widetilde{Q})\widetilde{P} \\ &+ (BB^T + AVX^T)Y + (BB^TV + AV\widetilde{P})\widetilde{Q}. \end{aligned}$$

From Theorem 1, we know that $\overline{\mathrm{grad} J_V} = (I - VV^T)R$. In order to apply Theorem 3, one can multiply the state equation of the system (2.8) by $\widehat{E}^{-1}$ from the left. However, in many engineering fields, the size of the system is very large, which leads to a larger error system. Then it may not be easy to perform the computation. Therefore, for the numerical efficiency, we are going to derive another expression for the ODE system.

Lemma 3. *If $\mathcal{P}$ and $\mathcal{Q}$ satisfy*

$$\mathcal{E}\mathcal{P}\mathcal{A}^T + \mathcal{A}\mathcal{P}\mathcal{E}^T + \mathcal{X} = 0 \quad \text{and} \quad \mathcal{E}^T\mathcal{Q}\mathcal{A} + \mathcal{A}^T\mathcal{Q}\mathcal{E} + \mathcal{Y} = 0,$$

then we can obtain $\mathrm{tr}(\mathcal{X}^T\mathcal{Q}) = \mathrm{tr}(\mathcal{Y}^T\mathcal{P})$.

Proof. Since $\mathcal{A}\mathcal{P}^T\mathcal{E}^T + \mathcal{E}\mathcal{P}^T\mathcal{A}^T + \mathcal{X}^T = 0$, it yields

$$\begin{aligned}\mathrm{tr}(\mathcal{X}^T\mathcal{Q}) &= -\mathrm{tr}(\mathcal{A}\mathcal{P}^T\mathcal{E}^T\mathcal{Q} + \mathcal{E}\mathcal{P}^T\mathcal{A}^T\mathcal{Q}) \\ &= -\mathrm{tr}(\mathcal{P}^T\mathcal{E}^T\mathcal{Q}\mathcal{A} + \mathcal{P}^T\mathcal{A}^T\mathcal{Q}\mathcal{E}) = \mathrm{tr}(\mathcal{P}^T\mathcal{Y}) = \mathrm{tr}(\mathcal{Y}^T\mathcal{P}).\end{aligned}$$

Thus, the proof of Lemma 3 is accomplished. □

Theorem 4. *Given the stable ODE system (2.4). $\widetilde{P}$ and $\widetilde{Q}$ are the controllability Gramian and the observability Gramian of the reduced system (2.5). X and Y satisfy (2.10) and (2.11), respectively. Then*

$$\overline{\mathrm{grad} J_V} = (I - VV^T)\widehat{R},$$

where

$$\begin{aligned}\widehat{R} :=& (-C^TC + A^TVY^TE + E^TVY^TA)X \\ &+ (C^TCV + A^TV\widetilde{Q}V^TEV + E^TV\widetilde{Q}V^TAV)\widetilde{P} \\ &+ (BB^T + AVX^TE^T + EVX^TA^T)Y \\ &+ (BB^TV + AV\widetilde{P}V^TE^TV + EV\widetilde{P}V^TA^TV)\widetilde{Q}.\end{aligned}$$

Proof. Since $J(V) = \mathrm{tr}(\widehat{C}\widehat{P}\widehat{C}^T)$, from the partitioning of $\widehat{P}$ and $\widehat{C}$, we have

$$J(V) = \mathrm{tr}(C^TC(P + V\widetilde{P}V^T - 2XV^T)).$$

For an arbitrary tangent vector $\xi \in T_{\mathcal{V}}Gr(r,n)$, there is a horizontal lift $\bar{\xi}_V \in T_VSt(r,n)$ such that $\xi = D\pi(V)[\bar{\xi}_V]$. Then

$$DJ(V)[\bar{\xi}_V] = DJ \circ \pi(V)[D\pi(V)[\bar{\xi}_V]] = DJ(\mathcal{V})[\xi].$$

Furthermore,

$$\begin{aligned}DJ(\mathcal{V})[\xi] = DJ(V)[\bar{\xi}_V] &= 2\mathrm{tr}(\bar{\xi}_V^T(C^TCV\widetilde{P} - C^TCX) \\ &+ \frac{1}{2}V^TC^TCVD\widetilde{P}[\bar{\xi}_V] - V^TC^TCDX[\bar{\xi}_V])).\end{aligned} \tag{4.1}$$

In order to replace $\mathrm{tr}(V^TC^TCVD\widetilde{P}[\bar{\xi}_V])$ and $-\mathrm{tr}(V^TC^TCDX[\bar{\xi}_V])$, by differentiating the both sides of (2.6) and (2.10), it yieds

$$\widetilde{E}D\widetilde{P}[\bar{\xi}_V]\widetilde{A}^T + \widetilde{A}D\widetilde{P}[\bar{\xi}_V]\widetilde{E}^T + M = 0, \tag{4.2}$$
$$EDX[\bar{\xi}_V]\widetilde{A}^T + ADX[\bar{\xi}_V]\widetilde{E}^T + N = 0, \tag{4.3}$$

where

$$\begin{aligned} M :=& \bar{\xi}_V^T EV\widetilde{P}V^TA^TV + V^TE\bar{\xi}_V\widetilde{P}V^TA^TV + V^TEV\widetilde{P}\bar{\xi}_V^TA^TV \\ &+ V^TEV\widetilde{P}V^TA^T\bar{\xi}_V + \bar{\xi}_V^TAV\widetilde{P}V^TE^TV + V^TA\bar{\xi}_V\widetilde{P}V^TE^TV \\ &+ V^TAV\widetilde{P}\bar{\xi}_V^TE^TV + V^TAV\widetilde{P}V^TE^T\bar{\xi}_V + \bar{\xi}_V^TBB^TV + V^TBB^T\bar{\xi}_V, \\ N :=& EX\bar{\xi}_V^TA^TV + EXV^TA^T\bar{\xi}_V + AX\bar{\xi}_V^TE^TV + AXV^TE^T\bar{\xi}_V + BB^T\bar{\xi}_V. \end{aligned}$$

Applying Lemma 3 to (4.2) and (2.7), we can obtain

$$\begin{aligned} \mathrm{tr}(V^TC^TCVD\widetilde{P}[\bar{\xi}_V]) =& \mathrm{tr}(\widetilde{Q}M) = 2\mathrm{tr}(\bar{\xi}_V^TEV\widetilde{P}V^TA^TV\widetilde{Q} + \bar{\xi}_V^TA^TV\widetilde{Q}V^TEV\widetilde{P} \\ &+ \bar{\xi}_V^TAV\widetilde{P}V^TE^TV\widetilde{Q} + \bar{\xi}_V^TE^TV\widetilde{Q}V^TAV\widetilde{P} + \bar{\xi}_V^TBB^TV\widetilde{Q}). \end{aligned} \tag{4.4}$$

Similarly, apply Lemma 3 to (4.3) and (2.11), and it yields

$$\begin{aligned} -\mathrm{tr}(V^TC^TCDX[\bar{\xi}_V]) &= \mathrm{tr}(Y^TN) \\ &= \mathrm{tr}(\bar{\xi}_V^TA^TVY^TEX + \bar{\xi}_V^TAVX^TE^TY \\ &\quad + \bar{\xi}_V^TE^TVY^TAX + \bar{\xi}_V^TEVX^TA^TY + \bar{\xi}_V^TBB^TY). \end{aligned} \tag{4.5}$$

Substituting (4.4) and (4.5) to (4.1), we can get

$$DJ(\mathcal{V})[\xi] = 2\mathrm{tr}(\bar{\xi}_V^T\widehat{R}).$$

According to the definition of the gradient and Theorem 1, the horizontal lift of $\mathrm{grad}J$ at V is

$$\overline{\mathrm{grad}J}_V = (I - VV^T)\widehat{R}.$$

Then, the proof of Theorem 4 is accomplished. □

Remark 3. When $E = I$, since $\bar{\xi}_V^TV = 0$, $\widehat{R}$ is naturally reduced to R. Then we generalize the existing H_2 optimal model reduction to the case $E \neq I$. In the next section, one can see that by the ε-embedding technique and the stable representation, our proposed model reduction method adapts to DAE systems and coupled systems.

Combining Theorem 2 and Theorem 4, the geodesic on $Gr(r,n)$ with the initial point $\mathcal{V}$ can be written as

$$\mathcal{V}(t) = \mathrm{span}(V\overline{V}\cos\overline{\Sigma}t + \overline{U}\sin\overline{\Sigma}t),$$

and $V(t) := (V\overline{V}\cos\overline{\Sigma}t + \overline{U}\sin\overline{\Sigma}t)\overline{V}^T$ belongs to $St(r,n)$, where $-\overline{\mathrm{grad}J}_V = \bar{U}\bar{\Sigma}\bar{V}^T$ is the thin SVD of $-\overline{\mathrm{grad}J}_V$. From the above analysis, we present a model reduction algorithm for the ODE system.

Algorithm 1 H_2 optimal model reduction of ODE systems on the Grassmann manifold

Input: The ODE system E, A, B, C, the initial reduced system $\widetilde{E}_0$, $\widetilde{A}_0$, $\widetilde{B}_0$, $\widetilde{C}_0$, and the iteration number n_0.
Output: The reduced system $\widetilde{E}$, $\widetilde{A}$, $\widetilde{B}$, $\widetilde{C}$.

for $i = 0$, $i = i + 1$, $i < n_0$ **do**
  Compute the matrices $\widetilde{P}_i$, $\widetilde{Q}_i$, X_i and Y_i from (2.6), (2.7), (2.10) and (2.11) with the subscript i.
  According to Theorem 4, Compute $\widehat{R}_i$.
  Compute the horizontal lift of the gradient at V_i as $\overline{\mathrm{grad}J}_{V_i} = (I - V_iV_i^T)\widehat{R}_i$.
  Let $H_i := -\overline{\mathrm{grad}J}_{V_i}$ be the search direction.
  Perform the thin SVD as $H_i = \overline{U}_i\overline{\Sigma}_i\overline{V}_i^T$.
  Minimize $J(V_i(t))$ over $t \geq 0$ where $V_i(t) = (V_i\overline{V}_i \cos\overline{\Sigma}_it + \overline{U}_i \sin\overline{\Sigma}_it)\overline{V}_i^T$ and set $t_i = t_{\min}$ and $V_{i+1} = V_i(t_i)$.
  $\widetilde{E}_{i+1} = V_{i+1}^TEV_{i+1}$, $\widetilde{A}_{i+1} = V_{i+1}^TAV_{i+1}$, $\widetilde{B}_{i+1} = V_{i+1}^TB$, $\widetilde{C}_{i+1} = CV_{i+1}$.
end for
return $\widetilde{E} = \widetilde{E}_{n_0}$, $\widetilde{A} = \widetilde{A}_{n_0}$, $\widetilde{B} = \widetilde{B}_{n_0}$, $\widetilde{C} = \widetilde{C}_{n_0}$.

In Algorithm 1, a step size t_i is needed to minimize $J(V_i(t))$. Here we present an inexact line-search method in the following remark [2].

Remark 4. A step size $t_i = \alpha\beta^j$ is termed as the Armijo step size if j is the smallest nonnegative integer such that

$$J(V_i) - J(V_i(\alpha\beta^j)) \geq -\alpha\beta^j\gamma\langle\overline{\mathrm{grad}J}_{V_i}, H_i\rangle,$$

where $\alpha > 0$, $\beta, \gamma \in (0, 1)$.

According to Algorithm 1, two model reduction algorithms for the coupled system are proposed in Section 5. One reduces the order of the closed-loop system, while the other constructs reduced subsystems to preserve the structure of the coupled system.

5 H_2 optimal model reduction of the coupled system on the Grassmann manifold

In this section, we focus on the model reduction of the coupled system. Based on Algorithm 1, two model reduction algorithms are presented.

Since the coupled system can be written as a closed-loop system, which has the same form as the system (2.4), Algorithm 1 can be employed to reduce the order of the closed-loop system. Regarding some DAE subsystems and unstable subsystems, there are two measures introduced in Section 3 to deal with.

For convenience, we assume that the first q subsystems are DAE subsystems with $\mathrm{rank}(E_j) = l_j < n_j$ for $j = 1, 2, \ldots, q$ and the last $k - q$ subsystems are ODE subsystems. In order to transform DAE subsystems into corresponding

ODE subsystems, we first embed the perturbation ε_j into the jth subsystem. It can be described as

$$E_j = U_j \begin{bmatrix} \Sigma_j & \\ & 0 \end{bmatrix} V_j^T \xRightarrow{\varepsilon_j} E_{\varepsilon_j,j} = U_j \begin{bmatrix} \Sigma_j & \\ & \varepsilon_j I_{n_j - l_j} \end{bmatrix} V_j^T. \tag{5.1}$$

We further assume that only the first obtained q subsystems are unstable. As stated in Section 3.2, we can find stable representations of these subsystems, and the matrices

$$\begin{aligned} K_{\text{new}} &= K\text{diag}\{[I_{m_1}, 0], \dots, [I_{m_q}, 0], I\} - \text{diag}\{[0, I_{p_1}], \dots, [0, I_{p_q}], 0\}, \\ R_{\text{new}} &= [R_1, 0, \dots, R_q, 0, R_{q+1}, \dots, R_k] \end{aligned} \tag{5.2}$$

and

$$A_{\text{new},j} = A_j + B_j F_j, \quad C_{\text{new},j} = \begin{bmatrix} C_j \\ F_j \end{bmatrix}, \quad j = 1, 2, \dots, q.$$

Let $\overline{B}_{\text{new}} = \overline{B}$ and

$$\begin{aligned} \overline{E}_{\text{new}} &= \text{diag}\{E_{\varepsilon_1,1}, \dots, E_{\varepsilon_q,q}, E_{q+1}, \dots, E_k\}, \\ \overline{A}_{\text{new}} &= \text{diag}\{A_{\text{new},1}, \dots, A_{\text{new},q}, A_{q+1}, \dots, A_k\}, \\ \overline{C}_{\text{new}} &= \text{diag}\{C_{\text{new},1}, \dots, C_{\text{new},q}, C_{q+1}, \dots, C_k\}. \end{aligned}$$

We construct the following closed-loop system

$$\begin{cases} E_{\text{new}} \dfrac{dx(t)}{dt} = A_{\text{new}} x(t) + B_{\text{new}} u(t), \\ y(t) = C_{\text{new}} x(t), \end{cases} \tag{5.3}$$

where $E_{\text{new}} = \overline{E}_{\text{new}}$, $A_{\text{new}} = \overline{A}_{\text{new}} + \overline{B}_{\text{new}} K_{\text{new}} \overline{C}_{\text{new}}$, $B_{\text{new}} = \overline{B}_{\text{new}} G$, and $C_{\text{new}} = R_{\text{new}} \overline{C}_{\text{new}}$. According to Section 3.1, E_{new} is a nonsingular matrix, and the system (5.3) is an approximation of the closed-loop system (2.3). Next, we present an algorithm to reduce the order of the system (5.3).

Algorithm 2 H_2 optimal model reduction of the closed-loop system on the Grassmann manifold

Input: The coefficient matrices of the coupled system (2.1) and (2.2), the perturbation ε_j, the reduced order r.

Output: The coefficient matrices of the reduced closed-loop system.

1: Embed the perturbation ε_j into the first q DAE subsystems as (5.1).
2: Find stable representations of unstable subsystems.
3: Construct the new closed-loop system (5.3).
4: Apply Algorithm 1 to the system (5.3) and obtain the transformation matrix V_c such that $V_c^T V_c = I_r$.
5: **return** $\widetilde{E}_{\text{new}} = V_c^T E_{\text{new}} V_c$, $\widetilde{A}_{\text{new}} = V_c^T A_{\text{new}} V_c$, $\widetilde{B}_{\text{new}} = V_c^T B_{\text{new}}$, $\widetilde{C}_{\text{new}} = C_{\text{new}} V_c$.

As one can see, even though the order of the coupled system is reduced, the obtained reduced system is an ODE system. In the next, we present an algorithm to construct reduced subsystems so that the coupled structure can be preserved.

Since the subsystems of the coupled system have the same form as the system (2.4), the methods introduced in Section 3 and the model reduction method proposed in Section 4 suit the subsystem (2.1). In order to apply Algorithm 1 to subsystems of coupled system, we firstly perform the ε-embedding technique on DAE subsystems as Section 3.1. Then regarding the stability, stable representations of unstable subsystems are constructed. Finally, Algorithm 1 is employed to obtain the reduced subsystems. Specific procedures are shown in the following Algorithm 3.

Algorithm 3 H_2 optimal model reduction of subsystems on the Grassmann manifold

---

Input: The coefficient matrices of the coupled system (2.1) and (2.2), the perturbation ε_j, the reduced order r.

Output: The reduced subsystems.

1: **if** The DAE subsystem is involved in the coupled system **then**
2:     Perform the ε-embedding technique.
3: **end if**
4: **if** The unstable subsystem is involved in the coupled system **then**
5:     Find the stable representation of the subsystem.
6: **end if**
7: Apply Algorithm 1 to the subsystems, which need to be reduced.
8: **return** The coefficient matrices of the reduced subsystems.

In the following, we present a comparison between Algorithm 2 and Algorithm 3. Since Algorithm 2 reduces the order of the closed-loop system, the size of the closed-loop system is obviously larger than that of every subsystem. It implies more computation may be needed. Moreover, the interconnected relations may be lost, for the coupled system is transformed into a closed-loop system before reduction. However, the H_2 optimality of the reduced system can be determined. By contrast, Algorithm 3 reduces the orders of subsystems. It costs relatively less computation than Algorithm 2. From Subsection 3.2, the reduced coupled system resulting from Algorithm 3 can retain the structure of the original coupled system, even though some subsystems are unstable. For the H_2 optimality, Algorithm 3 aims to form the H_2 optimal reduced subsystems, which can not generically ensure the H_2 optimality of the reduced coupled system. In addition, since to reduce the orders of subsystems can be individually performed, the parallelization is also an alternative way for Algorithm 3. In conclusion, when a reduced closed-loop system with the H_2 optimality is required, Algorithm 2 is a candidate. When we need a reduced coupled system, Algorithm 3 can be adopted.

6 Numerical examples

In this section, two numerical examples are employed to illustrate our proposed algorithms. Both numerical experiments are operated in Matlab R2010b. We compare our proposed algorithms with rational Krylov subspace model reduction methods and the IRKA method. The Krylov subspaces corresponding to transformation matrices are specified in the following examples. Some notations in these two examples are firstly introduced. *Original system*: the original coupled system. *System-1*: the reduced closed-loop system by rational Krylov subspace model reduction methods. *System-2*: the reduced closed-loop system by Algorithm 2. *System-3*: the reduced coupled system with the reduced subsystems by rational Krylov subspace model reduction methods. *System-4*: the reduced coupled system with the reduced subsystems by Algorithm 3. *System-5*: the reduced closed-loop system by the IRKA method. *System-6*: the reduced coupled system with the reduced subsystems by the IRKA method.

Example 1. The first model is an 1D heated beam with a PI-controller, which is introduced in [31]. The PI-controller is described as

$$\begin{cases} E_1 \dfrac{dx_1(t)}{dt} = A_1 x_1(t) + B_1 u_1(t), \\ y_1(t) = C_1 x_1(t), \end{cases}$$

where

$$E_1 = \begin{bmatrix} 1 & 0 \\ 0 & 0 \end{bmatrix}, \ A_1 = \begin{bmatrix} 0 & 0 \\ 0 & 1 \end{bmatrix}, \ B_1 = \begin{bmatrix} k_I \\ -k_P \end{bmatrix}, \ C_1 = \begin{bmatrix} 1 & 1 \end{bmatrix}.$$

The heat transfer along the beam is described as

$$\begin{aligned} &\frac{\partial T}{\partial t}(t,z) = \kappa \frac{\partial^2 T(t,z)}{\partial z^2}, \\ &\frac{\partial T}{\partial z}(t,0) = u_2(t), \qquad \frac{\partial T}{\partial z}(t,1) = 0. \end{aligned}$$

We measure the temperature at $z = 1$. After a spatial discretization of the PDE with $n_2 + 1$ equidistant grid points, the following system is obtained.

$$\begin{cases} E_2 \dfrac{dx_2(t)}{dt} = A_2 x_2(t) + B_2 u_2(t), \\ y_2(t) = C_2 x_2(t), \end{cases}$$

where $E_2 = I_{n_2}$,

$$A_2 = \kappa(n_2+1)^2 \begin{bmatrix} -1 & 1 & & & \\ 1 & -2 & 1 & & \\ & \ddots & \ddots & \ddots & \\ & & 1 & -2 & 1 \\ & & & 1 & -1 \end{bmatrix}, B_2 = \begin{bmatrix} \kappa(n_2+1) \\ 0 \\ \vdots \\ 0 \\ 0 \end{bmatrix}, C_2 = \begin{bmatrix} 0 \\ 0 \\ \vdots \\ 0 \\ 1 \end{bmatrix}^T.$$

The interconnected relations are expressed by

$$u_1(t) = u(t) - y_2(t), \quad u_2(t) = y_1(t), \quad y(t) = y_2(t).$$

Let $k_I = k_P = \kappa = 1$ and $n_2 = 1000$. Then the order of the coupled system is 1002. We generate the stable representations of the second subsystem and the closed-loop system. Let $E_{\text{new},\varepsilon} = \text{diag}\{1,\ 1,\ \cdots,\ 1,\ \varepsilon\}$ replace E_{new} with $\varepsilon = 10^{-10}$ and the feedback matrices

$$F_{\text{new}} = \big[-n_2 - 1, n_2 + 1, (n_2 + 1)^2, 0, \ldots, 0\big], \quad F_2 = \big[-n_2 - 1, 0, \ldots, 0\big],$$

such that $\lambda I - A_2 - B_2F_2$ and $\lambda E_{\text{new},\varepsilon} - A_{\text{new}} - B_{\text{new}}F_{\text{new}}$ are stable. Let r be the reduced order of the new closed-loop system (5.3) and r_2 be the reduced order of the second subsystem. The transformation matrices constructing System-1 and System-3 are the bases of $\mathrm{K}_{\frac{r}{2}}(A_{\text{new}}^{-T}E_{\text{new},\varepsilon}^T; A_{\text{new}}^{-T}[C_{\text{new}}^T\ F_{\text{new}}^T])$ and $\mathrm{K}_{r_2}(A_2^{-1}; A_2^{-1}B_2)$, respectively. In order to show the effectiveness of our proposed algorithms, the relative H_2 errors with different reduced orders compared to rational Krylov subspace model reduction methods are listed in Table 1. r is the order of the reduced closed-loop system, and the order of the reduced subsystem is r_2 satisfying $r = r_2 + 2$ such that the order of the reduced coupled system is equal to that of the reduced closed-loop system.

Table 1. Relative H_2 errors in Example 1.

r	4	6	8	10	12	14	16
System-1 ($\times 10^{-4}$)	4167	68.66	22.48	8.4126	2.8867	0.9584	0.9476
System-2 ($\times 10^{-4}$)	1381	66.83	20.00	4.8479	2.8003	0.7215	0.6306
r_2	2	4	6	8	10	12	14
System-3	0.9865	0.9437	0.8808	0.8050	0.7637	0.7638	0.7628
System-4	0.7354	0.3117	0.1143	0.0603	0.0225	0.0183	0.0125

Table 1 shows that System-2 and System-4 with different reduced orders have lower relative H_2 errors than System-1 and System-3, respectively. Table 2 lists the corresponding computational time of obtaining the reduced closed-loop systems and the reduced subsystems.

Table 2. Computational time (s) of obtaining reduced systems in Example 1.

r	4	6	8	10	12	14	16
System-1	0.8786	1.4019	1.8909	2.4258	3.0266	3.9049	4.5801
System-2	20.8192	17.1708	10.4067	22.4707	27.7424	33.8536	27.3245
r_2	2	4	6	8	10	12	14
System-3	0.7654	1.6088	2.6207	3.6675	4.9553	6.0995	7.2991
System-4	3.0097	4.8621	4.6398	10.7537	9.6225	9.2564	14.5050

Table 2 implies that rational Krylov subspace model reduction methods spend less time than our proposed algorithms in obtaining reduced systems. Algorithm 3 costs less time than Algorithm 2 to generate the reduced system.

Although rational Krylov subspace model reduction methods need less time to generate reduced systems, the reduced systems resulting from our proposed algorithms can better approximate the original system in the sense of the H_2 norm.

Example 2. We consider a delay differential system [24] as

$$\begin{cases} \dfrac{dx(t)}{dt} = -x(t-1) + u(t), \\ y(t) = x(t). \end{cases}$$

It can be interpreted as an interconnection of the subsystem

$$\begin{cases} \dfrac{dx_1(t)}{dt} = 0 \cdot x_1(t) + [\,1 \ \ -1\,] u_1(t), \\ y_1(t) = x_1(t) \end{cases}$$

and the pure unit delay $u_2(t) = u_2(t-1)$. The interconnected relations are

$$\begin{cases} u_1(t) = \begin{bmatrix} 0 \\ 1 \end{bmatrix} u_2(t) + \begin{bmatrix} 1 \\ 0 \end{bmatrix} u(t), \\ u_2(t) = y_1(t), \quad y(t) = y_1(t). \end{cases}$$

The delay can be achieved by the following PDE with boundary conditions:

$$\begin{aligned} &\frac{\partial f}{\partial t}(t,z) = \frac{\partial f}{\partial z}(t,z), \\ &f(t,0) = u_2(t), \quad f(t,1) = y_2(t). \end{aligned}$$

Through a spatial discretization of this equation with n_2 equidistant grid points, the pure unit delay can be approximated by

$$\begin{cases} \dfrac{dx_2(t)}{dt} = A_2 x_2(t) + B_2 u_2(t), \\ y_2(t) = C_2 x_2(t), \end{cases}$$

where

$$A_2 = n_2 \begin{bmatrix} -1 & 1 & & \\ & -1 & \ddots & \\ & & \ddots & 1 \\ & & & -1 \end{bmatrix}, \quad B_2 = \begin{bmatrix} 0 \\ 0 \\ \vdots \\ n_2 \end{bmatrix}, \quad C_2 = \begin{bmatrix} 1 \\ 0 \\ \vdots \\ 0 \end{bmatrix}^T.$$

Let $n_2 = 1000$, and a coupled system of the order $n = 1001$ is obtained. In order to find a stable representation of the first subsystem, we choose $F_1 = [0, 2]^T$. The transformation matrices constructing System-1 and System-3 are the bases of $\mathrm{K}_r(A_{\text{new}}^{-T}; A_{\text{new}}^{-T} C_{\text{new}}^T)$ and $\mathrm{K}_{r_2}(A_2^{-1}; A_2^{-1} B_2)$ respectively. In order to show the effectiveness of our proposed algorithms, the relative H_2 errors with different reduced orders compared to rational Krylov subspace model reduction methods are listed in Table 3. r is the order of the reduced closed-loop system, and the order of the reduced subsystem is r_2 satisfying $r = r_2 + 1$.

Table 3. Relative H_2 errors in Example 2.

r	2	4	6	8	10	12	14
System-1	0.3032	0.0192	0.0072	0.0037	0.0026	0.0026	0.0022
System-2	0.0789	0.0188	0.0071	0.0035	0.0020	0.0013	8.297×10^{-4}
System-5	0.0782	0.0151	0.0057	0.0028	0.0015	8.69×10^{-4}	5.154×10^{-4}
r_2	1	3	5	7	9	11	13
System-3	0.9867	0.9481	0.9048	0.8586	0.8105	0.7612	0.7113
System-4	0.9797	0.9004	0.8215	0.7615	0.6703	0.5925	0.5264
System-6	–	–	0.9424	0.7876	0.6432	0.5128	0.3990

Table 3 shows that System-2 and System-4 with different reduced orders entirely have lower relative H_2 errors than System-1 and System-3, respectively. Table 4 presents the computational time of obtaining the reduced closed-loop systems with the order r and the reduced subsystems with the order r_2.

Table 4. Computational time (s) of obtaining reduced systems in Example 2.

r	2	4	6	8	10	12	14
System-1	0.6234	1.4657	2.4116	3.4448	4.5206	5.6688	6.8196
System-2	6.2947	8.9342	10.9433	13.3053	13.4730	14.9436	15.7148
System-5	27.3285	24.5133	23.9021	25.0187	24.3174	23.8584	25.6909
r_2	1	3	5	7	9	11	13
System-3	0.2629	0.9408	1.9271	2.7280	3.7189	4.7935	6.0180
System-4	2.7510	7.2980	7.5772	12.2098	12.5839	13.4629	13.7329
System-6	–	–	8.7395	8.9385	8.9861	8.9291	9.2615

From Table 4, rational Krylov subspace model reduction methods cost least time to form the reduced systems. Compared with the IRKA method, Algorithm 2 spends less time in reducing the closed-loop system. Next, we present the bode frequency responses of the original system, System-1, System-2, System-3 and System-4. The order of the reduced closed-loop system is 44, while that of the reduced subsystem is 43.

According to Figures 1 and 2, the reduced systems can approximate the original system well in the frequency domain except that System-1 exhibits little derivation. Finally, we reduce the order of the second subsystem to $r_2 = 42$, and present the transient responses of the subsystem and the reduced systems in $[0,\ 1.5]$ with the input $u(t) = \mathrm{e}^{-t}\sin(\pi t + 1)$. The initial condition $x_2(0)$ is chosen as

$$x_2(0) = [\,\underbrace{1\,1\,\ldots\,1}_{900}\,\underbrace{0\,0\,\ldots\,0}_{100}\,],$$

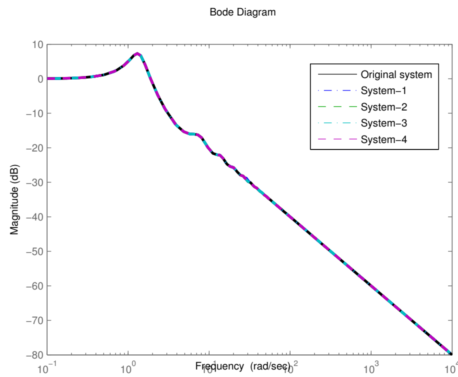

Figure 1. Magnitude in Example 2

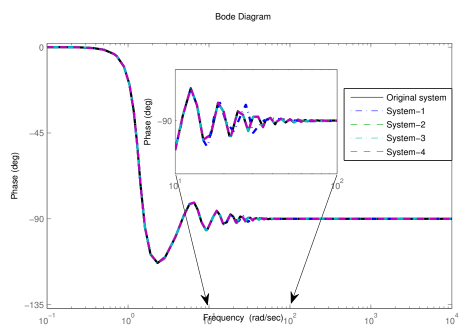

Figure 2. Phase in Example 2

and the initial conditions of reduced subsystems are $V_{21}^T x_2(0)$ and $V_{22}^T x_2(0)$, where V_{21} and V_{22} are the transformation matrices corresponding to these two reduced subsystems.

Figures 3 and 4 show that System-4 can provide a better approximation than System-3 in this case. Combining with the relative H_2 errors, computational time, frequency responses and transient responses, we conclude that our proposed algorithms are feasible.

Conclusions

In this paper, the H_2 optimal model reduction methods for coupled systems with unstable subsystems are investigated. H_2 optimal model reduction of ODE systems on the Grassmann manifold is mainly explored. By introducing the ε-embedding technique and the stable representation, an unstable DAE system can be changed into a coupled system with stable ODE subsystems. Then

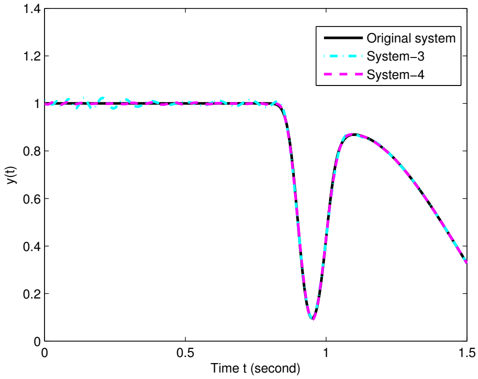

Figure 3. Transient responses in Example 2

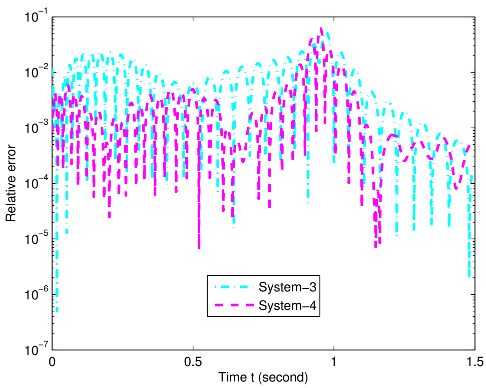

Figure 4. Relative errors in Example 2

based on the form of the subsystems and the closed-loop system, the model reduction method is generalized to coupled systems and two corresponding model reduction algorithms are established. Finally, numerical examples demonstrate the approximation results.

References

[1] P.A. Absil, R. Mahony and R. Sepulchre. Riemannian geometry of Grassmann manifolds with a view on algorithmic computation. *Acta Appl. Math.*, **80**(2):199–220, 2004. https://doi.org/10.1023/B:ACAP.0000013855.14971.91.

[2] P.A. Absil, R. Mahony and R. Sepulchre. *Optimization Algorithms on Matrix Manifolds*. Princeton University Press, Princeton, 2009.

[3] A.C. Antoulas. *Approximation of Large-Scale Dynamical Systems.* SIAM, Philadelphia, 2005.

[4] A. Bunse-Gerstner, R. Byers, V. Mehrmann and N.K. Nichols. Feedback design for regularizing descriptor systems. *Linear Algebra Appl.*, **299**(1-3):119–151, 1999. https://doi.org/10.1016/S0024-3795(99)00167-6.

[5] C.Y. Chen, Y.L. Jiang and H.B. Chen. An ε-embedding model-order reduction approach for differential-algebraic equation systems. *Math. Comp. Model. Dyn. Syst.*, **18**(2):223–241, 2012. https://doi.org/10.1080/13873954.2011.614258.

[6] P.V. Dooren, K.A. Gallivan and P.A. Absil. H_2-optimal model reduction with higher-order poles. *SIAM J. Matrix Anal. Appl.*, **31**(5):2738–2753, 2010. https://doi.org/10.1137/080731591.

[7] A. Edelman, T.A. Arias and S.T. Smith. The geometry of algorithms with orthogonality constraints. *SIAM J. Matrix Anal. Appl.*, **20**(2):303–353, 1998. https://doi.org/10.1137/S0895479895290954.

[8] S. Gugercin, A.C. Antoulas and C. Beattie. $\mathcal{H}_2$ model reduction for large-scale linear dynamical systems. *SIAM J. Matrix Anal. Appl.*, **30**(2):609–638, 2008. https://doi.org/10.1137/060666123.

[9] S. Gugercin, T. Stykel and S. Wyatt. Model reduction of descriptor systems by interpolatory projection methods. *SIAM J. Sci. Comput.*, **35**(5):B1010–B1033, 2013. https://doi.org/10.1137/130906635.

[10] G. Jankevičiūtė, T. Leonavičienė, R. Čiegis and A. Bugajev. Reduced order models based on Pod method for Schröinger equations. *Math. Model. Anal.*, **18**(5):694–707, 2013. https://doi.org/10.3846/13926292.2013.870611.

[11] Y.L. Jiang. *Model Order Reduction Methods.* Science Press, Beijing, 2010.

[12] Y.L. Jiang, C.Y. Chen and H.B. Chen. Model-order reduction of coupled DAE systems via ε-embedding technique and Krylov subspace method. *J. Franklin Inst.*, **349**(10):3027–3045, 2012. https://doi.org/10.1016/j.jfranklin.2012.09.004.

[13] Y.L. Jiang and H.B. Chen. Application of general orthogonal polynomials to fast simulation of nonlinear descriptor systems through piecewise-linear approximation. *IEEE Trans. Comput. Aided Design*, **31**(5):804–808, 2012. https://doi.org/10.1109/TCAD.2011.2179879.

[14] Y.L. Jiang and H.B. Chen. Time domain model order reduction of general orthogonal polynomials for linear input-output systems. *IEEE Trans. Automat. Control*, **57**(2):330–343, 2012. https://doi.org/10.1109/TAC.2011.2161839.

[15] Y.L. Jiang and K.L. Xu. H_2 optimal reduced models of general MIMO LTI systems via the cross gramian on the stiefel manifold. *J. Franklin Inst.*, **354**(8):3210–3224, 2017. https://doi.org/10.1016/j.jfranklin.2017.02.019.

[16] A.I. Klimushchev and N.N. Krasovskii. Uniform asymptotic stability of systems of differential equations with a small parameter in the derivative terms. *J. Appl. Math. Mech.*, **25**(4):1011–1025, 1961. https://doi.org/10.1016/S0021-8928(61)80009-9.

[17] Z. Luo. A POD-based reduced-order stabilized Crank-Nicolson MFE formulation for the non-stationary parabolized Navier-Stokes equations. *Math. Model. Anal.*, **20**(3):346–68, 2015. https://doi.org/10.3846/13926292.2015.1048758.

[18] C. Magruder, C. Beattie and S. Gugercin. Rational krylov methods for optimal L_2 model reduction. In *49th IEEE Conference on Decision and Control (CDC)*, pp. 6797–6802, USA, 2010. IEEE.

[19] V. Mehrmann and T. Stykel. Balanced truncation model reduction for large-scale systems in descriptor form. In P. Benner, V. Mehrmann and D.C. Sorensen(Eds.), *Dimension Reduction of Large-Scale Systems*, pp. 83–115. Springer, 2005.

[20] H.K.F. Panzer, T. Wolf and B. Lohmann. H_2 and H_∞ error bounds for model order reduction of second order systems by krylov subspace methods. In *2013 European Control Conference (ECC)*, pp. 4484–4489, France, 2013. IEEE.

[21] Z.Z. Qi, Y.L. Jiang and Z.H. Xiao. Time domain model order reduction using general orthogonal polynomials for K-power bilinear systems. *Int. J. Control*, **89**(5):1065–1078, 2016. https://doi.org/10.1080/00207179.2015.1117659.

[22] S. Rajamanickam. *Efficient algorithms for sparse singular value decomposition.* Diss. University of Florida, 2009.

[23] T. Reis. Circuit synthesis of passive descriptor systems–a modified nodal approach. *Int. J. Circ. Theor. Appl.*, **38**(1):44–68, 2010. https://doi.org/10.1002/cta.532.

[24] W.H.A. Schilders, H.A. Van der Vorst and J. Rommes. *Model Order Reduction: Theory, Research Aspects and Applications.* Springer, Berlin, 2008.

[25] K. Sinani. *Iterative Rational Krylov Algorithm for Unstable Dynamical Systems and Genaralized Coprime Factorizations.* Diss. Virginia Tech, 2016.

[26] T. Stykel. On some norms for descriptor systems. *IEEE Trans. Automat. Control*, **51**(5):842–847, 2006. https://doi.org/10.1109/TAC.2006.875010.

[27] A. Varga. Computation of coprime factorizations of rational matrices. *Linear Algebra Appl.*, **271**(1-3):83–115, 1998. https://doi.org/10.1016/S0024-3795(97)00256-5.

[28] P. Vuillemin, C. Poussot-Vassal and D. Alazard. H_2 optimal and frequency limited approximation methods for large-scale LTI dynamical systems. In E. Witrant, J. Martinez-Molina, M. Lovera, O. Sename and L. Dugard(Eds.), *5th IFAC Symposium on System Structure and Control*, volume 46 of *IFAC Proceedings Volumes*, pp. 719–724, France, 2013. Elsevier.

[29] P. Vuillemin, C. Poussot-Vassal and D. Alazard. Poles residues descent algorithm for optimal frequency-limited H_2 model approximation. In *2014 European Control Conference (ECC)*, pp. 1080–1085, France, 2014. IEEE.

[30] P. Vuillemin, C. Poussot-Vassal and D. Alazard. Spectral expression for the frequency-limited H_2-norm of LTI dynamical systems with high order poles. In *2014 European Control Conference (ECC)*, pp. 55–60, France, 2014. IEEE.

[31] X.L. Wang and Y.L. Jiang. Model order reduction methods for coupled systems in the time domain using Laguerre polynomials. *Comput. Math. Appl.*, **62**(8):3241–3250, 2011. https://doi.org/10.1016/j.camwa.2011.08.039.

[32] W.Y. Yan and J. Lam. An approximate approach to H_2 optimal model reduction. *IEEE Trans. Automat. Control*, **44**(7):1341–1358, 1999. https://doi.org/10.1109/9.774107.